High-Temperature Tensile Creep Behavior of A [001] Orientation Single Crystal Nickel-Base Superalloy

Y. Su,^{1,2} S. G. Tian,^{2,*} L. L. Yu,² H. C. Yu,³ S. Zhang² and B. J. Qian²

- ¹ College of Mechanical Engineering, Shenyang University of Chemical Technology, 110142 Shenyang, China
- ² School of Materials Science and Engineering, Shenyang University of Technology, 110870 Shenyang, China
- ³ Beijing Institute of Aeronautical Material, 100095 Beijing, China

Abstract. By means of the measurement of creep curves and microstructure observation, an investigation has been made into the microstructure evolution of γ phase in [001] orientation single crystal nickel-base superalloy during tensile creep. Results show that, after full heat treatment, the microstructure of the single crystal nickel-base superalloy consists of the cubical γ' phase embedded coherently in the γ matrix, and arranged regularly along the (100) orientations. During tensile creep, the cubical γ phase in the alloy is transformed into the rafted structure along the direction vertical to the applied stress axis. During steady state creep, the strain rate of the single crystal nickel-base superalloy is controlled by the climbing of dislocations in the ranges of the applied temperatures and stresses. After crept up to fracture, various morphologies of the rafted γ' phase are displayed in different regions of the specimen, and the coarsening and twist extent of the rafted γ' phase increase as the distance from the fracture decreases, which is attributed to the increment of the effective stress and strain extent in the necked region.

Keywords. Single crystal nickel-base superalloy, tensile creep, microstructure evolution.

PACS® (2010). 81.40.Lm.

1 Introduction

Single crystal nickel-base superalloys have been widely used in hot-end components like aeroengine turbine blades

Corresponding author: S. G. Tian, School of Materials Science and Engineering, Shenyang University of Technology, 110870 Shenyang, China; E-mail: tiansugui2003@gmail.com.

Received: October 26, 2010. Accepted: November 12, 2010.

due to their excellent high-temperature mechanical properties. The microstructure of single crystal nickel-base superalloys consists of the cubic γ phase embedded coherently in the γ matrix phase, of which the γ phase is the strengthening phase [1-3]. Some experimental results show that the high-temperature creep behavior of single crystal nickelbase superalloys has close relationships with the evolution features of γ phase [4,5]. Better mechanical properties may be obtained when the γ phase occupies a higher volume fraction. During high-temperature service, the centrifugal force acted on the blade parts may result in the evolution of γ' phase, namely, the initial cubical γ' phase in the alloy is transformed into the rafted structure [6]. Understanding the evolution features of γ phase may predict the service lifetime of the blade parts served at high temperatures [7]. Although several investigations have reported the influence of the rafted γ'/γ phases structure on the creep properties of single crystal nickel-base superalloys, and some literatures have reported the microstructure evolution regularity of γ' phase in the single crystal nickel-base superalloys [8,9], the influencing effects of the microstructure evolution and them on creep features of single crystal nickel-base superalloys are still unclear.

In this paper, the microstructure evolution of γ' phase in [001] orientation single crystal nickel-base superalloy is investigated by means of the measurement of creep curves and microstructure observation of the alloy crept under different conditions.

2 Materials and Methods

A [001] orientation single crystal nickel-base superalloy has been produced by means of selecting a crystal method in a vacuum directional solidification furnace under a high temperature gradient. The specimen was within 3° deviating from [001] orientation. The nominal chemical composition of the superalloy is Ni-9.0Cr-5.0W-5.5Al-4.5Co-1.7Ti (wt. %). The heat treatment regimes of the specimens are given as follows: 1523 K, 4 h; AC + 1143 K, 32 h; AC.

After full heat treatment, the specimen was machined into the plate-like tensile creep specimen along [001] orientation, the schematic diagram of the specimen is shown in Figure 1. After the specimen surface was mechanically ground and polished, a uni-axial constant load tensile testing was performed in a creep testing machine (GWT504 model), and creep curves under the experimental condi-

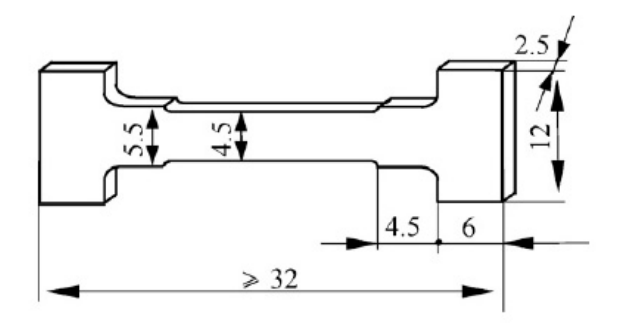


Figure 1. Schematic diagram of creep specimen (unit: mm).

tions were measured. Then the samples before and after crept for different time were etched by the solution of 20 g CuSO₄ + 5 ml H₂SO₄ + 100 ml HCl + 80 ml H₂O to observe the microstructure under SEM. Additionally, the microstructures and morphologies of $\gamma\prime$ phase in different regions of the superalloy during creep up to fracture were observed.

3 Experimental Results and Analysis

3.1 Creep Features of the Alloy

Creep curves of the single crystal nickel-base superalloy under different conditions have been measured, as shown in Figure 2. The creep curves of the alloy under the applied stress of 137 MPa at different temperatures are shown in Figure 2(a), indicating that the alloy displays a lower strain rate and the longer creep lifetime at 1313 K, and the strain rate of the alloy during the steady state creep is measured to be 0.009214 %/h. With the temperature elevated to 1345 K, the strain rate of the alloy during steady state creep increases to 0.023971 %/h, the lasting time of the alloy during the steady state creep is about 93 h, and the creep lifetime of the alloy is measured to be 115 h. Moreover, the creep lifetime of the alloy decreases to 98 h with the temperature further elevated to 1353 K. After crept for 380 h under the applied stress of 137 MPa at 1313 K (see Figure 2(b)), the fact that the alloy still maintains in the period of the steady state creep indicates that the alloy displays an obvious sensibility to the applied temperatures.

Creep curves of the alloy under the applied different stresses at 1313 K are shown in Figure 2(b), which indicates that the alloy displays a relatively short initial creep stage and relatively long steady state creep stage under the applied stress of 160 MPa, the strain rate of the alloy during the steady state creep is measured to be 0.009646 %/h, and the creep lifetime of the alloy is about 257 h. But the creep lifetime of the alloy decreases to 98 h as the applied stress increases to 180 MPa. This indicates that the alloy displays an obvious sensibility on the applied stress when the applied stress is over 160 MPa.

3.2 Constitutive Creep Equation and Creep Parameters

The primary strain of the single crystal superalloy during creep occurs at the moment of applying stress. As the creep goes on, the strain of the alloy increases and the strain rate decreases. When the creep of the alloy enters the steady state stage, the strain rate of the alloy maintains constant, and the rate equation may be expressed by Dorn creep law given as follows [10]:

$$\dot{\varepsilon}_{\rm ss} = A \, \sigma_A^n \exp\left(-\frac{Q}{RT}\right). \tag{1}$$

In the equation, $\dot{\varepsilon}_{\rm ss}$ is the strain rate during the steady state creep, A the constant related to material structure, σ_A the applied stress, n the apparent stress exponent, R the gas constant, T thermodynamics temperature, and Q apparent active energy.

According to the data in Figure 2, the strain rates of the alloy during steady state creep under different conditions can be measured. And the dependence of the strain rate during the steady state creep on the applied temperatures and stresses are shown in Figure 3. Therein, the relationship between the strain rate and the applied temperatures is shown in Figure 3(a), and in the ranges of the applied temperatures and stresses, the apparent creep active energy of the alloy is measured to be Q=469.56 kJ/mol. According to the relationship between the strain rates and the applied stresses as shown in Figure 3(b), the apparent stress exponent of the alloy is measured to be n=4.77. It can be deduced according to the data that the strain rate of the alloy during steady state creep is controlled by the climbing of dislocations in the range of the applied temperatures and stresses.

3.3 Microstructure Evolution of the Alloy During Creep

After fully heat treated, the microstructure of the alloy consists of the cubical $\gamma\prime$ phase embedded coherently in the γ matrix phase, as shown in Figure 4. The normal of the observing specimen is [100] orientation. The dark regions in Figure 4 are the $\gamma\prime$ phase, and the gray regions are the γ matrix phase. It is indicated from Figure 4 that the $\gamma\prime$ phase on (100) crystal plane displays the cubical morphology, the average edge length of the cubical $\gamma\prime$ phase is about 0.4 μ m, the width of γ matrix channel is about 50 nm, and arranged regularly along $\langle 100 \rangle$ orientation. The morphologies of the $\gamma\prime$ phase on (001) and (010) crystal planes are similar to that on (100) crystal plane (the photos omitted).

Figure 5 shows the morphologies of the [001] orientation superalloy crept for different time at 1313 K/160 MPa. It indicates that, after crept for 5 h, the cubical $\gamma\prime$ phase in the alloy is gradually being transformed into the rafted structure, the sizes of the $\gamma\prime$ and γ matrix phases in thickness are about 0.4 and 0.2 μ m, respectively, but some cubical $\gamma\prime$ precipitates are still reserved in the alloy as marked by the arrow in Figure 5(a). After crept for 30 h, the side channel

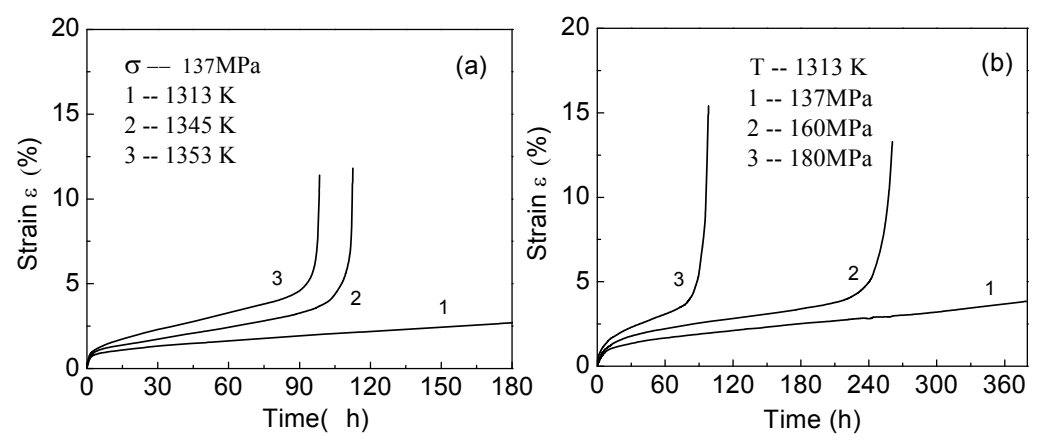


Figure 2. Creep curves of the single crystal nickel-base superalloy under different conditions. (a) applied stress of 137 MPa at different temperatures, (b) applied different stresses at 1313 K.

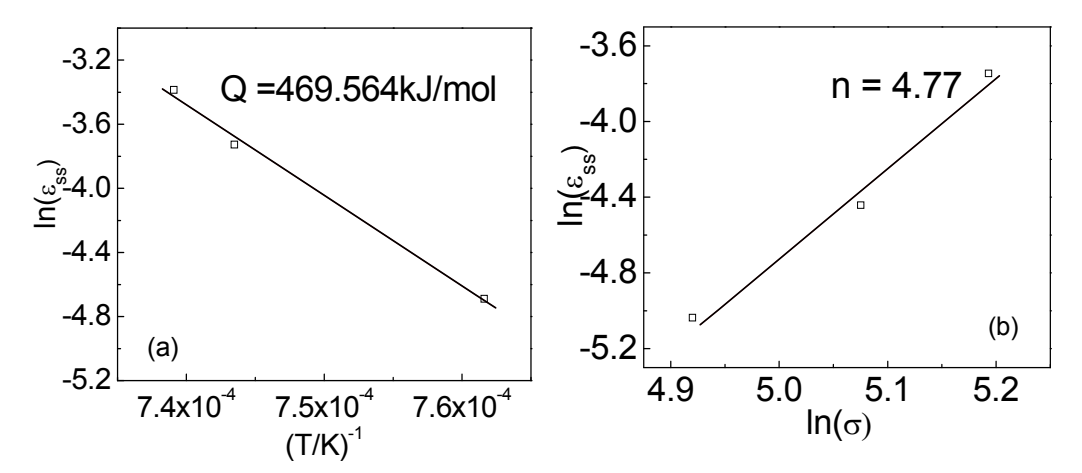


Figure 3. Relationship between the strain rate and the applied temperatures/stresses during the steady state creep. (a) dependence of the strain rate on temperatures at 137 MPa, (b) dependence of the strain rate on applied stresses at 1313 K.

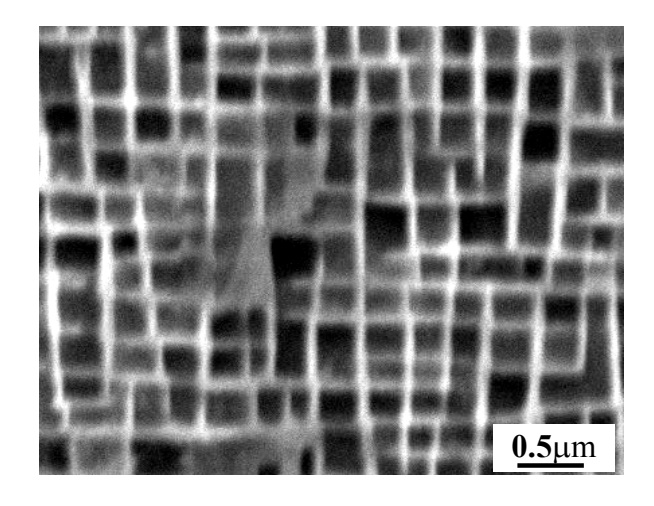


Figure 4. Morphology after the alloy fully heat treated.

near the $\gamma\prime$ phase has disappeared, and the $\gamma\prime$ phase is transformed into the rafted structure along the direction vertical to the applied stress axis, as shown in Figure 5(b), and the sizes of the $\gamma\prime$ and γ matrix phases in thickness increase to 0.6 and 0.4 μ m, respectively. After crept for 257 h, the morphology of the rafted $\gamma\prime$ phase near the fracture is shown in Figure 5(c), from which it can be seen that the coarsening of the rafted $\gamma\prime$ phase occurs, and the sizes of the $\gamma\prime$ and γ phases in thickness further increase to about 1 and 0.8 μ m, respectively. Additionally, the twist of the rafted $\gamma\prime$ phase occurs in the region near the fracture for displaying the wavy morphology due to the bigger plastic deformation.

During creep at constant load, the various stresses are applied in the different region in the specimen, which results in the various morphologies displayed in the different regions far from or near the fracture. Therefore, the deformed extent in the different regions of specimen may be evaluated according to the morphologies in the different regions of the specimen for investigating the influence of the applied stress on the morphology evolution of the alloy.

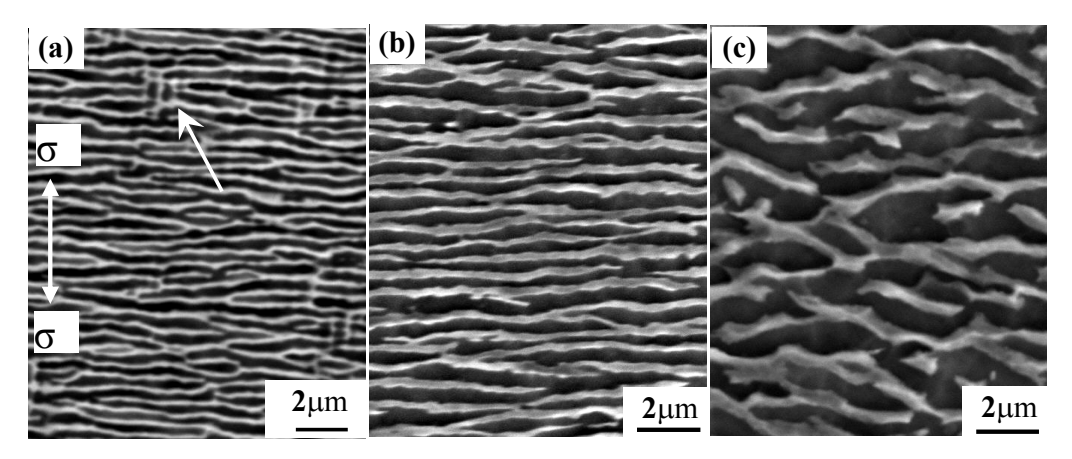


Figure 5. Morphologies of the superalloy crept for different time at 1313 K/160 MPa. (a) crept for 5 h, (c) crept for 30 h, (d) crept for 257 h up to fracture.

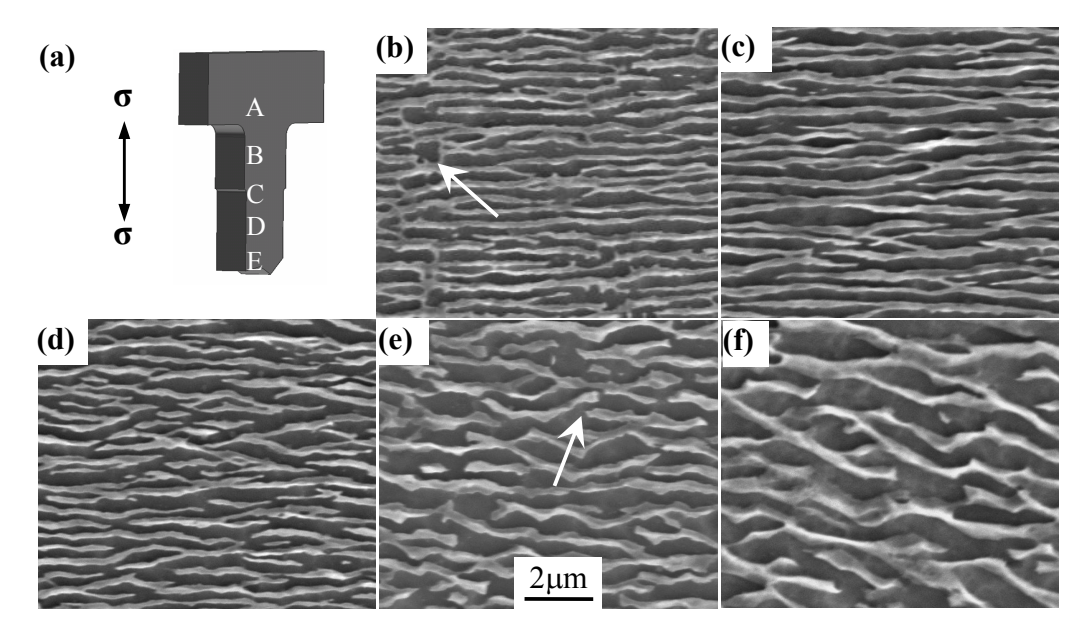


Figure 6. Morphologies of the rafted γ' phase in different regions of the single crystal nickel-base superalloy crept up to fracture at 1313 K/160 MPa. Schematic diagram of marking locations on specimen, (b), (c), (d), (e), (f) being SEM morphologies corresponding to the regions A, B, C, D and E, respectively.

After the alloy is crept for 257 h up to fracture at 1313 K/160 MPa, the morphologies of the rafted $\gamma\prime$ phase in the different regions of the specimen are shown in Figure 6. The schematic diagram of marking the observed locations on the specimen is shown in Figure 6(a). the stressfree region in the specimen is marked by letter A, where the $\gamma\prime$ phase is linked to form the rafted structure along the direction vertical to the stress axis as shown in Figure 6(b), but some coarser cubical $\gamma\prime$ phase are still reserved as marked by the white arrow. The $\gamma\prime$ phase in the regions B and C has completely been transformed into the rafted structure along the direction vertical to the stress axis, and the coarsening of the $\gamma\prime$ phase occurs as shown in Figure 6(c) and (d).

Though the $\gamma\prime$ phase in the region D still displays the rafted structure, the coarsening of the rafted $\gamma\prime$ phase occurs obviously: the size of the rafted $\gamma\prime$ phase in thickness increases to about 0.8 μ m, and the rafted $\gamma\prime$ phase displays the twisted configuration in which the coarser rafted $\gamma\prime$ phase is broken as marked by the arrow in Figure 6(e). The morphology of the rafted $\gamma\prime$ phase near the fracture is shown in Figure 6(f), indicating that rafted $\gamma\prime$ phase in the region displays the coarser twisted configuration which is not vertical to the direction of the stress axis, and the inclined degree relative to the stress axis increases with the decrease of the distance from the fracture. It is indicated by analysis that the deformation degree of the specimen near the fracture

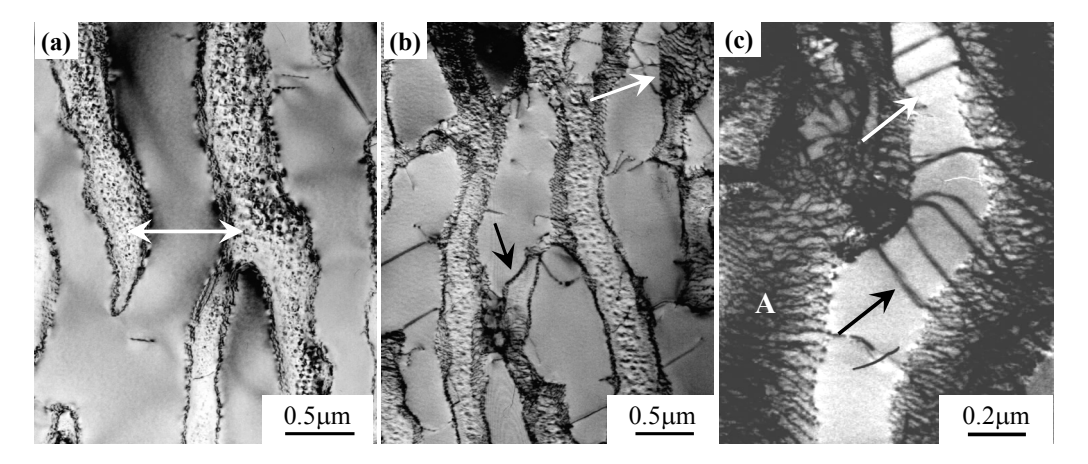


Figure 7. Microstructures of the [001] orientation alloy crept for different time at 1313 K/160 MPa. (a) crept for 80 h, (b) crept for 257 h up to fracture in the middle region, (c) morphology near the fracture region.

increases as the creep goes on, which results in the twist of the rafted γ / phases up to the break of them.

It is considered by analysis from the phenomena mentioned above that the microstructure evolution of the alloy is related to the applied stress values and strain extent of the alloy. As the creep goes on, the strain value of the alloy during creep increases, and when it reaches a certain value, the necking phenomenon occurs in middle regions of the specimen, which causes the increase of the effective stress of the applied constant loading and the coarsening of the rafted γ' phase. At the same time, the alternant slipping of the creep dislocations occurs, which results in the twist of the rafted γ' phase. As the strain values in the necked region further increases, the crystal rotation in the region occurs [11], which can change the original orientation of the rafted γ' phase.

3.4 Deformation Feature of the Alloy During Creep

Microstructures of the [001] orientation superalloy crept for different time at 1313 K/160 MPa are shown in Figure 7. Figure 7(a) shows the microstructure of the alloy crept for 80 h, which indicates that the original cubic γ' phase has been transformed into the rafted structure along the direction vertical to the stress axis (the direction of the applied stress is marked by the white double-headed arrow in the figure) when the creep of the alloy enters the steady state stage, and significant amount of the fine γ' phases are precipitated within the γ matrix channels. The fact that no dislocations shearing into the γ' phase are detected indicates that the deformation mechanism of the alloy during the steady state creep is thought to be the dislocation climbing over the γ' raft phase.

The microstructure of the alloy crept for 257 h up to fracture under the applied stress of 160 MPa at 1313 K is shown in Figure 7(b), indicating that the size of the rafted γ / phase in thickness is about 0.7–0.9 μ m. For the posi-

tion is far away from the fracture region, there are only few $\langle 110 \rangle$ super-dislocations shearing into the rafted $\gamma \prime$ phase as marked by the black arrow, and the interfacial dislocations appear in between the rafted γ' and γ phases as marked by the white arrow. Figure 7(c) shows the microstructure near the rupture region of the alloy. It can be seen that, at the latter stage of creep, the dislocation network formed during creep has been destroyed, which results in large amounts of dislocations shearing into the γ phase. From the figure it can also be seen that the various configurations of the dislocations are displayed in the different regions, of which significant amount of dislocations networks or tangles appear in the region of the $\gamma l/\gamma$ phases interfaces as marked by letter A. The parallel dislocations are activated in the rafted γ phase as marked by the arrows, and the direction of the parallel dislocations on the upside is vertical to that of the parallel dislocations on the downside in Figure 7(c). Consequently, it can be deduced that at the latter stage of creep, the various configurations of the dislocations shear into the rafted γ phase, which manifests that the creep resistance of the alloy has disappeared.

4 Conclusions

- 1. The microstructure of the [001] orientation single crystal nickel-base superalloy with the misorientation of 3° consists of the cubical γ' phase embedded coherently in the γ matrix, and arranged regularly along the $\langle 100 \rangle$ orientations. During tensile creep, the γ' phase is transformed into the rafted structure along the direction normal to that of the applied tensile stress axis.
- 2. The strain rate of the [001] orientation single crystal nickel-base superalloy during steady state creep is controlled by the climbing of dislocations in the range of the applied temperatures and stresses. At the latter stage of creep, many groups of dislocations have sheared into the

rafted $\gamma\prime$ phase, which manifests that the creep resistance has disappeared.

3. After crept up to fracture, the various morphologies of the rafted $\gamma\prime$ phase are displayed in the different regions of the alloy. The deformation extent of the specimen increases as the distance from the fracture decreases, and the size of the rafted $\gamma\prime$ phase in thickness and the twist extent also increase. Moreover, the crystal rotation occurs in the necked region of the specimen as the strain values further increases, which may result in the coarsening and twist of the rafted $\gamma\prime$ phase to change the original orientation.

References

- [1] W. Y. Ma, S. S. Li, M. Qiao, S. K. Gong, Y. R. Zheng and Y. F. Han, *Chin. J. Nonferrous Met.*, **16** (2006), 937.
- [2] Z. P. Luo, Z. T. Wu and D. J. Miller, *Mater. Sci. Eng. A*, 354 (2003), 358.

- [3] Z. Q. Hu, L. R. Liu, T. Jin and X. F. Sun, Aeroengine, 31 (2005), 1.
- [4] I. Toru, T. Katsushi, H. Adachi, K. Kishida, N. L. Okamoto, H. Inui, T. Yokokawa and H. Harada, *Acta Mater.*, 57 (2009), 1078
- [5] K. Y. Cheng, C. Y. Jo, T. Jin and Z. Q. Hu, *Mater. Des.*, 31 (2010), 968.
- [6] S. G. Tian, J. H. Zhang, Y. B. Xu, Z. Q. Hu, H. C. Yang and X. WU, *Mater. Sci. Eng. A*, 32 (2001), 2947.
- [7] P. Y. Wei, Z. Zhong, C. Li, S. Liu, Z. Yang and X. Cheng, J. Aeronaut. Mater., 19 (1999), 7.
- [8] X. F. Yu, S. G. Tian, H. Q. Du, H. C. Yu, M. G. Wang, L. J. Shang and S. S. Cui, *Mater. Sci. Eng. A*, **506** (2009), 80.
- [9] S. G. Tian, C. R. Chen, H. C. Yang and Z. Q. Hu, Acta Metall. Sin., 36 (2000), 465.
- [10] A. K. Mukherjee, J. E. Bird and J. E. Dorn, *Trans. ASM.*, 62 (1969), 155.
- [11] X. P. Guo, H. Z. Fu and J. H. Sun, Acta Metall. Sin., 30 (1994), 321.